PNAS
www.pnas.org

Supplementary Information for

A balance between vector survival and virus transmission is achieved through JAK/STAT signaling inhibition by a plant virus

Yu-Meng Wang[a,b,c], Ya-Zhou He[d,e], Xin-Tong Ye[a,b,c], Tao Guo[a,b,c], Li-Long Pan[a,b,c], Shu-Sheng Liu[a,b,c], James C. K. Ng[f], Xiao-Wei Wang[a,b,c,1]

[a]State Key Laboratory of Rice Biology, Zhejiang University, Hangzhou 310058, China; [b]Ministry of Agriculture Key Lab of Molecular Biology of Crop Pathogens and Insects, Zhejiang University, Hangzhou 310058, China; [c]Key Laboratory of Biology of Crop Pathogens and Insects of Zhejiang Province, Zhejiang University, Hangzhou 310058, China; [d]Key Laboratory of Integrated Pest Management on Crops in East China (MARA), Nanjing Agricultural University, Nanjing 21095, China; [e]College of Plant Protection, Nanjing Agricultural University, Nanjing 21095, China; and [f]Department of Microbiology and Plant Pathology, University of California, Riverside, CA 92521

[1]Xiao-Wei Wang
Email: xwwang@zju.edu.cn

This PDF file includes:

Supplementary Text

Materials and Methods

Insects, viruses and plants

A population of Middle East Asia Minor 1 (MEAM1) (mitochondrial cytochrome oxidase I GenBank accession no. GQ332577), a putative species of the *B. tabaci* complex was used in the present study. Whiteflies were reared on cotton plants (*Gossypium hirsutum* L. cv. Zhemian 1793) in insect-proof cages at 26 ± 1°C under a photoperiod of 14:10 h (light/dark) and a relative humidity of 60% (± 10%). The purity of the population was monitored every three generations by amplifying and sequencing the mitochondrial cytochrome oxidase I gene, which has been widely used to differentiate *B. tabaci* genetic groups. Infectious clones of TYLCV isolate SH2 (GenBank accession no. AM282874) were agro-inoculated into 3-4 true leaf stage tomato (*Solanum lycopersicum* cv. Hezuo 903) plants, and the plants were used approximately 3-4 weeks post virus inoculation. All plants were grown in insect-proof greenhouses under a controlled temperature of 25 ± 3°C and natural lighting.

Yeast two-hybrid (Y2H) assay

Y2H assay was performed using the Matchmaker Gold Yeast Two-Hybrid System (Clontech) and Yeastmaker Yeast Transformation System 2 (Clontech) as described in the manufacturer's instructions. A cDNA library of *B. tabaci* was constructed in the prey plasmid, Sfi I digested pGADT7, using the SMART cDNA library construction kit (Clontech). The bait vector, pGBKT7-TYLCV CP, was constructed by fusing the full-length TYLCV CP into pGBKT7 with *EcoRI.* Y2H Gold yeast cells were co-transformed with pGBKT7-TYLCV CP and the *B. tabaci* cDNA library. Positive clones were selected in the quadruple dropout medium (SD/-Leu/-Trp/-His/-Ade). Plasmids from the positive clones were recovered, and transformed into *Escherichia coli* strain DH5α and sequenced thereafter. To further confirm the interaction, we co-transformed the bait and prey plasmids into yeast and repeated the selection on the quadruple dropout media with X-α-Gal and 200 ng/ml Aureobasidin A.

Antibody preparation

The sequence corresponding to the N-terminal 200 amino acids of BtSTAT was amplified and constructed into the pET28a expression vector (Novagen) for fusion with a His tag. Primers used for the construction are listed in *SI Appendix*, Table S2. The recombinant protein His-BtSTAT$_{1\text{-}200}$ was purified using Ni Sepharose (GE Healthcare) following the manufacturer's instructions and served as antigen to produce rabbit anti-BtSTAT polyclonal antibody (HUABIO Co., Ltd.). The specificity of the BtSTAT antibody was validated in HEK293 cells over-expressing BtSTAT (*SI Appendix*, Fig. S10*A*).

Tissue collection

The midguts were dissected from the abdomen in pre-chilled PBS buffer and PSGs were dissected from the prothorax. The midguts and PSGs were washed twice in PBS to remove contamination from the hemolymph. For hemolymph collection, 10 whiteflies were dissected from the abdomen in 10 μL pre-chilled PBS buffer to release the content. After that, all the liquid containing hemolymph together with hemocytes was collected.

Q(RT)-PCR analysis

For viral DNA quantification in whiteflies, groups of 20 whiteflies were ground in 40 µL of ice-cold lysis buffer (50 mM Tris-HCl with pH at 8.4, 0.2% gelatin, 0.45% Tween 20, 0.45% Nonidet P-40, and 60 mg/L proteinase K) and incubated at 65°C for 2 h, and then at 100°C for 10 min. The supernatants were kept at - 20°C. For absolute quantification of TYLCV DNA in plants, dilution series containing between 10 and 10^8 copies of circular dsDNA pcDNA3.1 carrying a full-length *CP* gene of TYLCV were used as quantification standards. The number of TYLCV DNA molecules was calculated according to the generated standard curve. Gene transcription analyses were performed to measure the *Bt*STAT expression levels in each of the following (in groups of 100): midguts, primary salivary glands and hemolymph of non-viruliferous whiteflies, and groups of 40 whiteflies were used for gene expression level determination in whitefly whole bodies. Total RNA was isolated using TRIzol reagent (Ambion) and cDNAs were synthesized using the PrimeScript RT reagent kit with gDNA Eraser (TaKaRa), all according to the manufacturer's instructions. Q(RT)-PCR was performed on the CFX Connect Real-Time PCR System (Bio-Rad) with the SYBR Premix Ex TaqTM II (TaKaRa). A negative control (nuclease-free water) was included throughout the experiments to spot contamination and to determine the degree of primer-dimer formation. All primers used are listed in *SI Appendix*, Table S2. The amplification efficiency of primers for qPCR are listed in *SI Appendix*, Table S3. The relative gene expression or relative abundance of viral DNA was calculated using the $2^{-\Delta Ct}$ method and normalized to the *B. tabaci* β-*actin* gene.

Immunofluorescence assay

Midguts dissected from female whiteflies were fixed in 4% paraformaldehyde (MultiSciences Biotech) for 1 h at room temperature and washed three times in TBST (Tris-buffered saline [TBS] buffer with 0.05 % Tween 20). Afterward, the specimens were permeabilized using 0.1% Triton X-100 in TBS and blocked in TBST containing 1% BSA for 2 h at room temperature, followed by overnight incubation with anti-TYLCV CP monoclonal antibody (1:500) in TBST containing 1% BSA at 4°C, and then with goat anti-mouse (1:500) secondary antibody labeled with Dylight 549 in TBST containing 1% BSA for 1 h at room temperature, with extensive washing in between antibody applications. After the final wash, the midguts were mounted in fluoroshield mounting medium with DAPI (Abcam) and imaged using fluorescence microscopy.

Image acquisition and processing

Fluorescence images were captured using a Zeiss LSM710 confocal microscope. Dylight 549-labeled antibody and nuclear DNA were visualized using a 561-nm laser and a 405-nm laser for excitation, respectively. The control and experimental images were acquired and processed in the same fashion. Maximum intensity projection images were generated using the ZEN 2012 (blue edition) digital imaging system. For fluorescence density quantification, a single in-focus plane was acquired and analyzed using the ImageJ software. Immunoblotting images were captured using the chemiluminiscence imaging system (Bio-Rad), and the density of protein was determined using ImageJ.

Statistical analysis

Data were presented as mean ± SEM of three independent biological replicates, unless otherwise noted. One-way ANOVA followed by least significant difference test was applied for multiple

comparisons. For comparison of whitefly survival and virus transmission efficiency, percentage data were arcsine square root transformed. Differences among fluorescence densities in midguts were analyzed by the non-parametric Mann-Whitney *U* test. The others were assessed with an independent-sample *t* test. All analyses were performed using the SPSS 13.0 statistics software.

Supplementary Figures

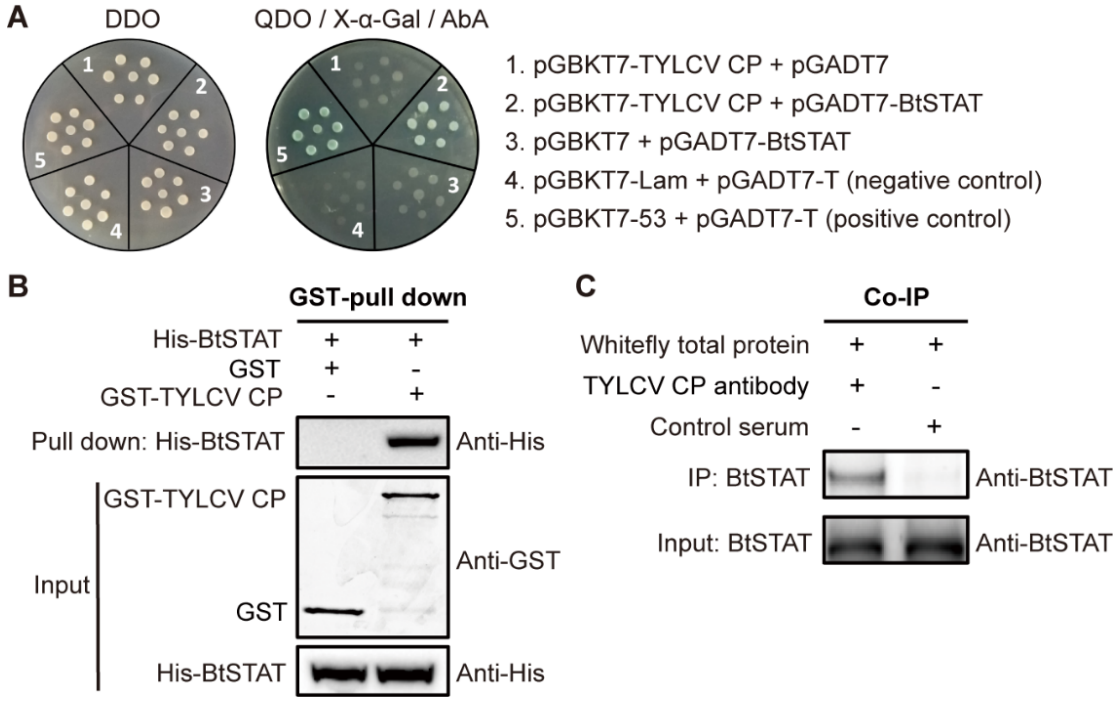

Fig. S1. TYLCV coat protein (CP) interacts with whitefly STAT. (A) The interaction between TYLCV CP and BtSTAT in yeast. Yeast strain Y2H Gold co-transformed with the indicated plasmids was spotted on DDO and QDO with X-α-gal and AbA. (B) GST-tag pull down assay. Recombinant BtSTAT interacted with GST-fused TYLCV CP. The products from GST vector (pGEX-6p-1) were applied as negative control. Anti-His and anti-GST antibodies were used to detect proteins. (C) Co-immunoprecipitation (Co-IP) of BtSTAT with anti-TYLCV CP monoclonal antibody in whitefly crude extracts.

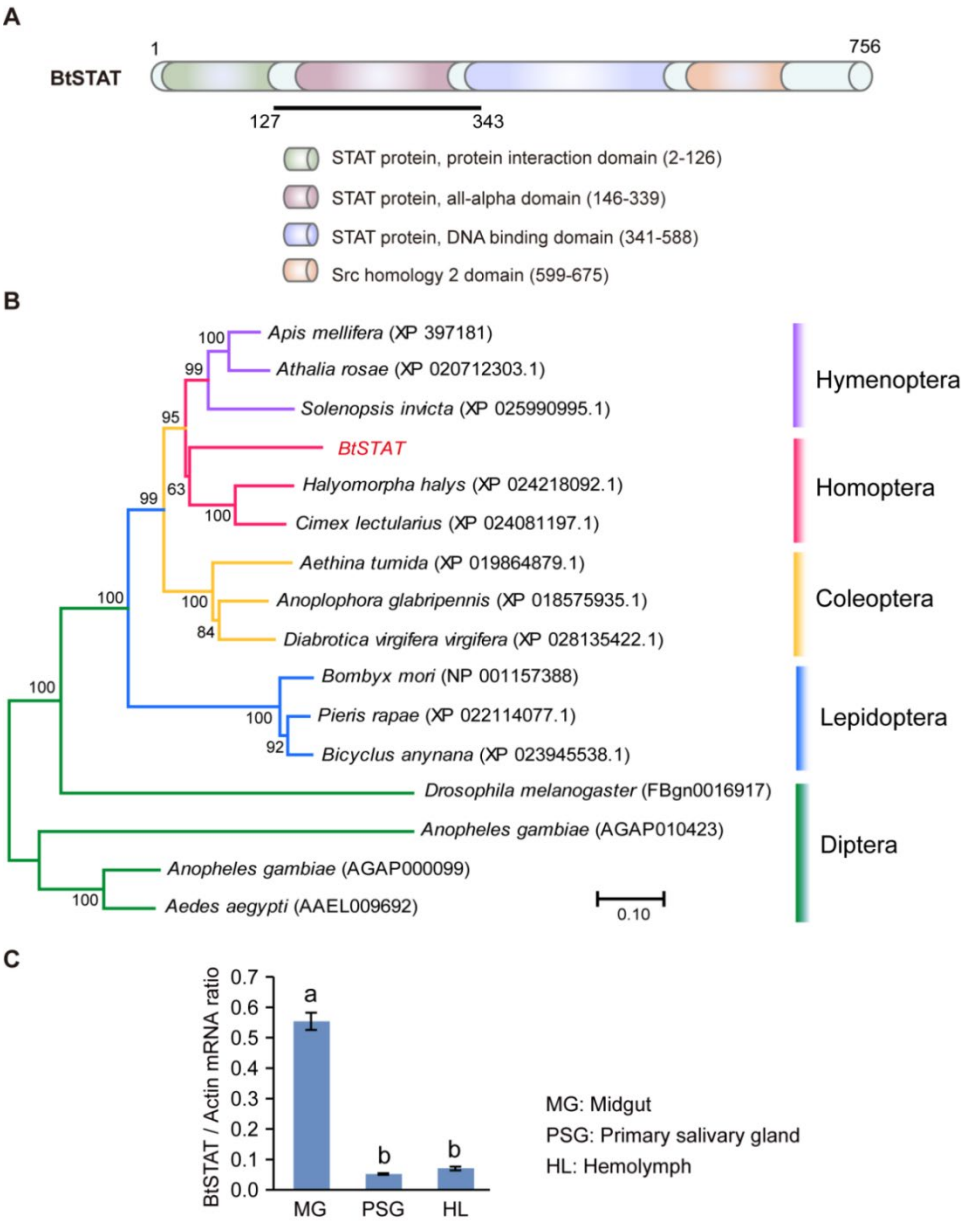

Fig. S2. Structural, phylogenetic and expression analysis of *Bemisia tabaci* STAT (BtSTAT). (A) Schematic diagram showing the domain composition of BtSTAT (GenBank accession no. MN058988). Conserved domains were predicted using the SMART database (http://smart.embl-heidelberg.de/). The black line indicates the partial STAT sequence identified by yeast two-hybrid assay. (B) A phylogenetic tree of STATs from different insects. The phylogenetic tree was constructed using the neighbor-joining algorithm (MEGA7.0.14) from full sequence alignments computed in ClustalX. Bootstrap analysis (1000 replicates) was applied to evaluate the internal support for the tree topology. (C) Relative transcript levels of *BtSTAT* in various tissues of non-viruliferous whiteflies. Mean ± SEM from three independent experiments with 100 midguts, 100 primary salivary glands and hemolymph from 100 whiteflies in each replicate. $p < 0.05$ (one-way ANOVA, LSD test).

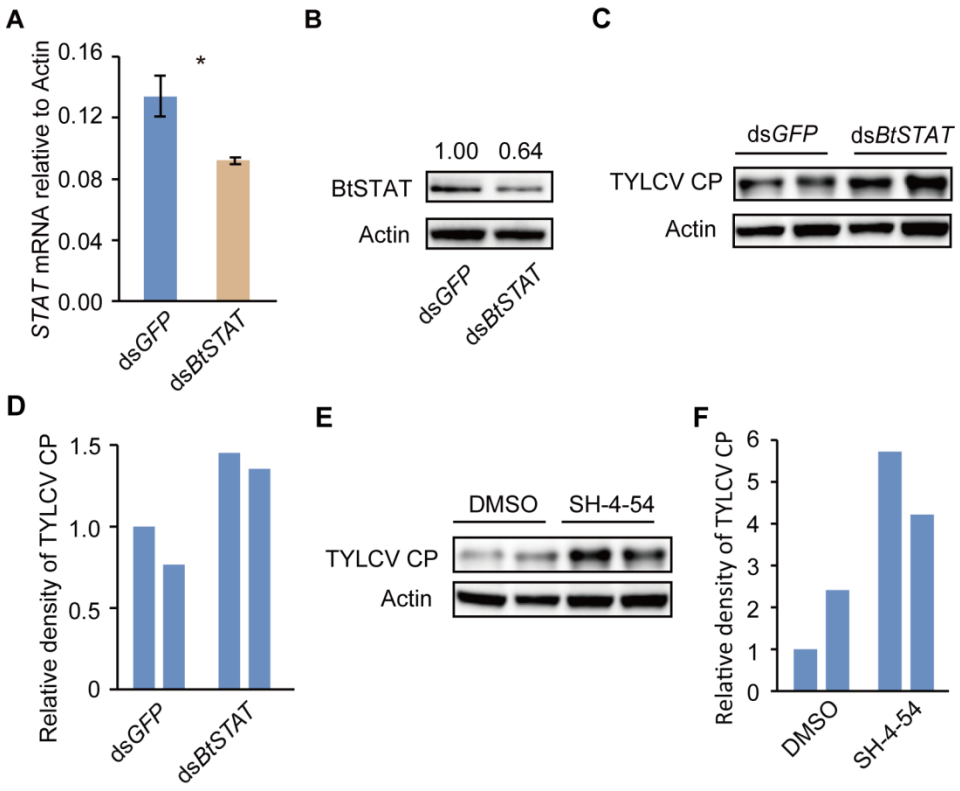

Fig. S3. Effect of BtSTAT deficiency on TYLCV CP accumulation in whitefly. (A and B) The relative mRNA levels (A) and protein levels (B) of *BtSTAT* in whiteflies after feeding with ds*GFP* or ds*BtSTAT*. Mean ± SEM from three independent experiments with 40 whiteflies in each replicate. **p* < 0.05 (independent-samples *t* test). The relative densities of BtSTAT were normalized with those of Actin. (C and D) Immunoblot analysis of TYLCV CP in whiteflies that were fed with ds*GFP* or ds*BtSTAT* for 48 h following a 48-h AAP on TYLCV-infected plants. (E and F) Immunoblot analysis of TYLCV CP in whiteflies that were fed with DMSO or SH-4-54 (prepared in DMSO) for 48 h following a 48-h AAP on TYLCV-infected plants. (C-F) The relative densities of TYLCV CP were normalized with those of Actin.

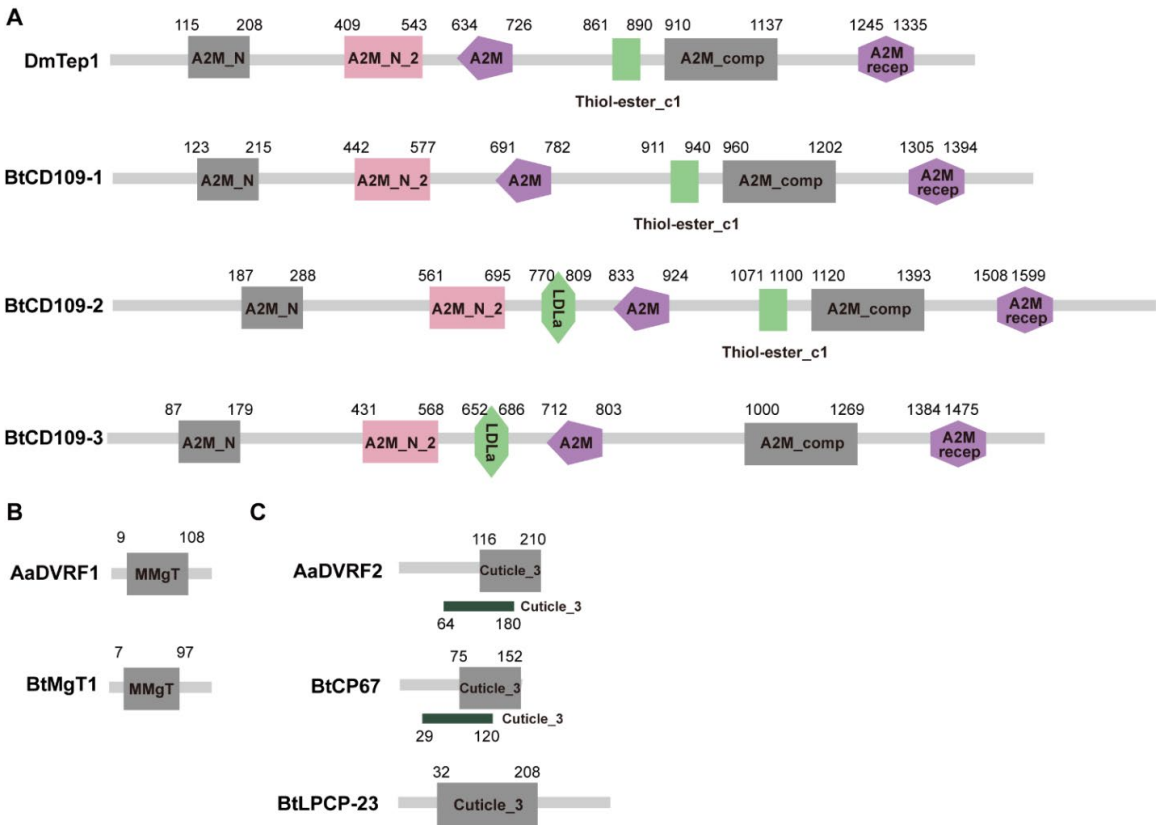

Fig. S4. Schematic diagram showing the domain composition of *Drosophila melanogaster* Tep1 (DmTep1), BtCD109-1/-2/-3 (A), *Aedes aegypti* DVRF1 (AaDVRF1), BtMgT1 (B), *A. aegypti* DVRF2 (AaDVRF2), BtCP67 and BtLPCP-23 (C). The conserved functional domains were predicted using the SMART database.

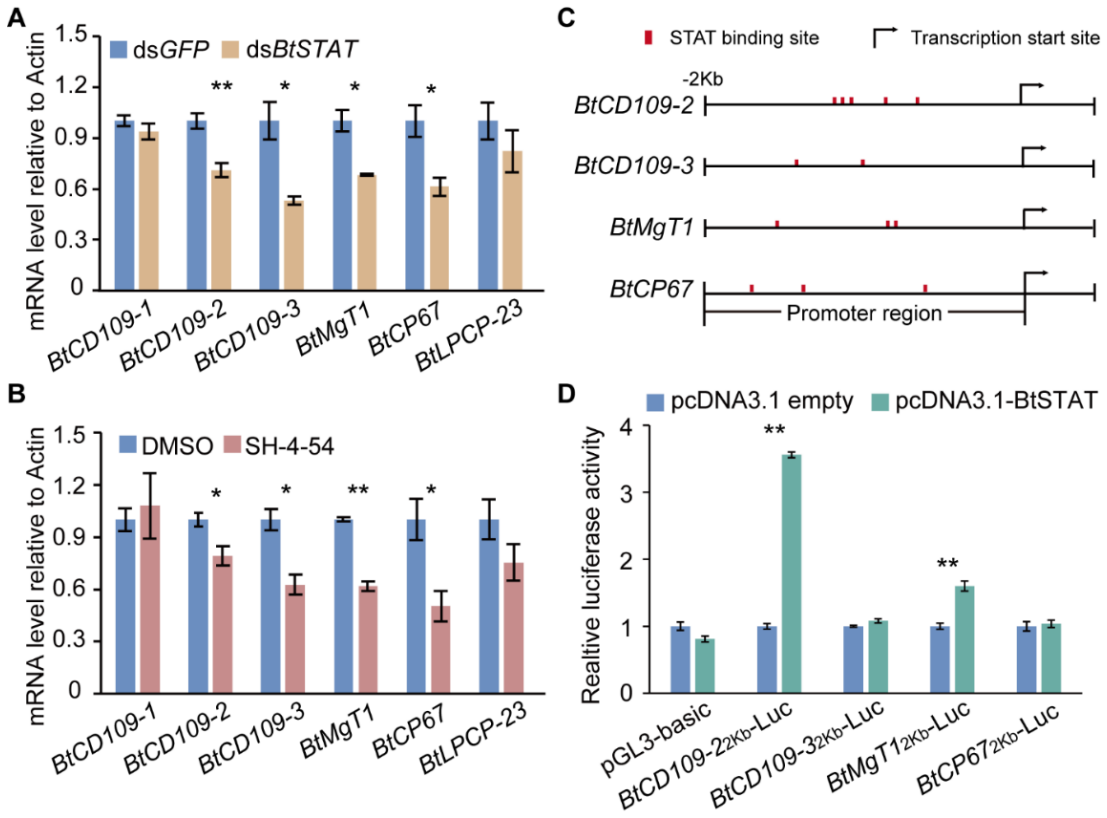

Fig. S5. Identification of downstream genes regulated by BtSTAT. (A and B) Relative mRNA levels of putative BtSTAT downstream genes in non−viruliferous whiteflies after dsRNA (A) or STAT inhibitor (B) treatment. Mean ± SEM from three independent experiments with 40 whiteflies in each replicate. *$p < 0.05$, **$p < 0.01$ (independent-samples *t* test). (C) Predicted STAT-binding sites in the promoter regions of the four BtSTAT-regulated genes. The 2-kb DNA sequence upstream of the transcription start site of each gene was analyzed by JASPAR (http://jaspar.genereg.net/). The red boxes indicate the locations of the predicted STAT-binding sites. (D) Luciferase assays in HEK293 cells transfected with the expression vector for BtSTAT (pcDNA3.1-BtSTAT), the desired reporter construct as indicated, and a *Renilla* luciferase reporter construct as internal reference. Treatments with empty expression vector (pcDNA3.1 empty) served as negative controls. Data represent normalized luciferase activity (firefly/*Renilla*) and are shown as mean ± SEM from four independent experiments. *$p < 0.05$, **$p < 0.01$ (independent-samples *t* test).

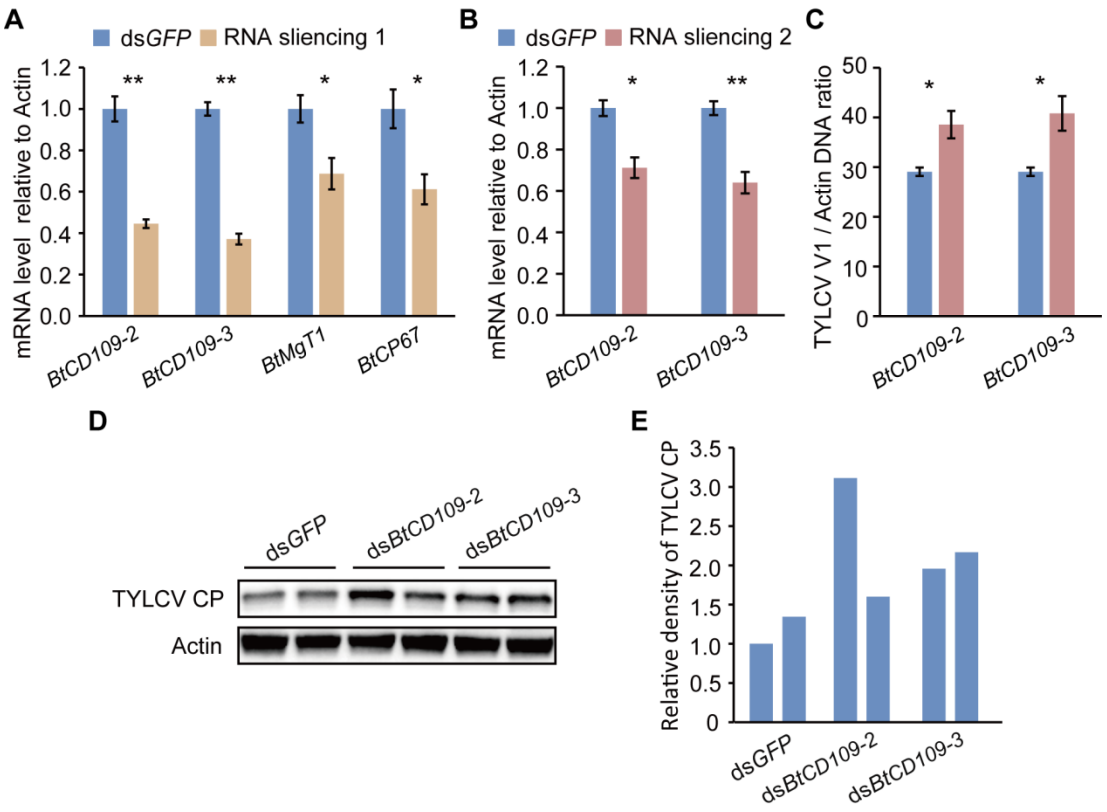

Fig. S6. Effect of BtSTAT-regulated genes silencing on TYLCV CP accumulation in whitefly. (A) The relative mRNA levels of BtSTAT-regulated genes in whiteflies after feeding with the corresponding dsRNA. (B) The relative mRNA levels of *BtCD109-2* or *-3* in whiteflies after feeding with another ds*BtCD109-2* or *-3*. (C) Quantitative analysis of TYLCV DNA in whiteflies that were fed with another ds*BtCD109-2* or *-3* for 48 h following a 48-h AAP on TYLCV-infected plants. (D and E) Immunoblot analysis of TYLCV CP in whiteflies that were fed with dsRNAs for 48 h following a 48-h AAP on TYLCV-infected plants. The relative densities of TYLCV CP were normalized with those of Actin. (A-C) Mean ± SEM from three independent experiments with 40 (A and B) or 20 (C) whiteflies in each replicate. *$p < 0.05$, **$p < 0.01$ (independent-samples *t* test).

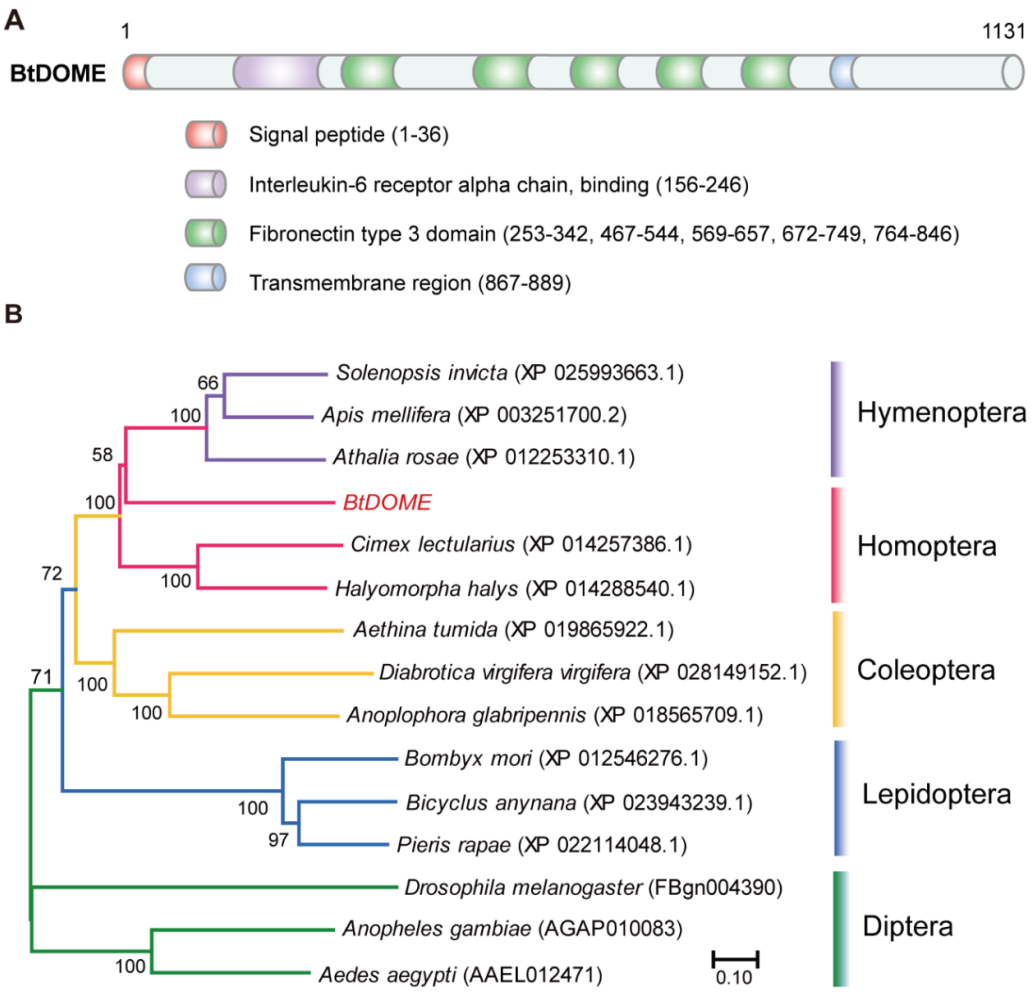

Fig. S7. Structural and phylogenetic analysis of BtDOME. (A) Schematic diagram showing the domain composition of BtDOME (Bta07497). The conserved domains were predicted using the SMART database. (B) Phylogenetic tree of DOMEs from different insects. The phylogenetic tree was constructed using the neighbor-joining algorithm (MEGA7.0.14) from full sequence alignments computed in ClustalX. Bootstrap analysis (1000 replicates) was applied to evaluate the internal support for the tree topology.

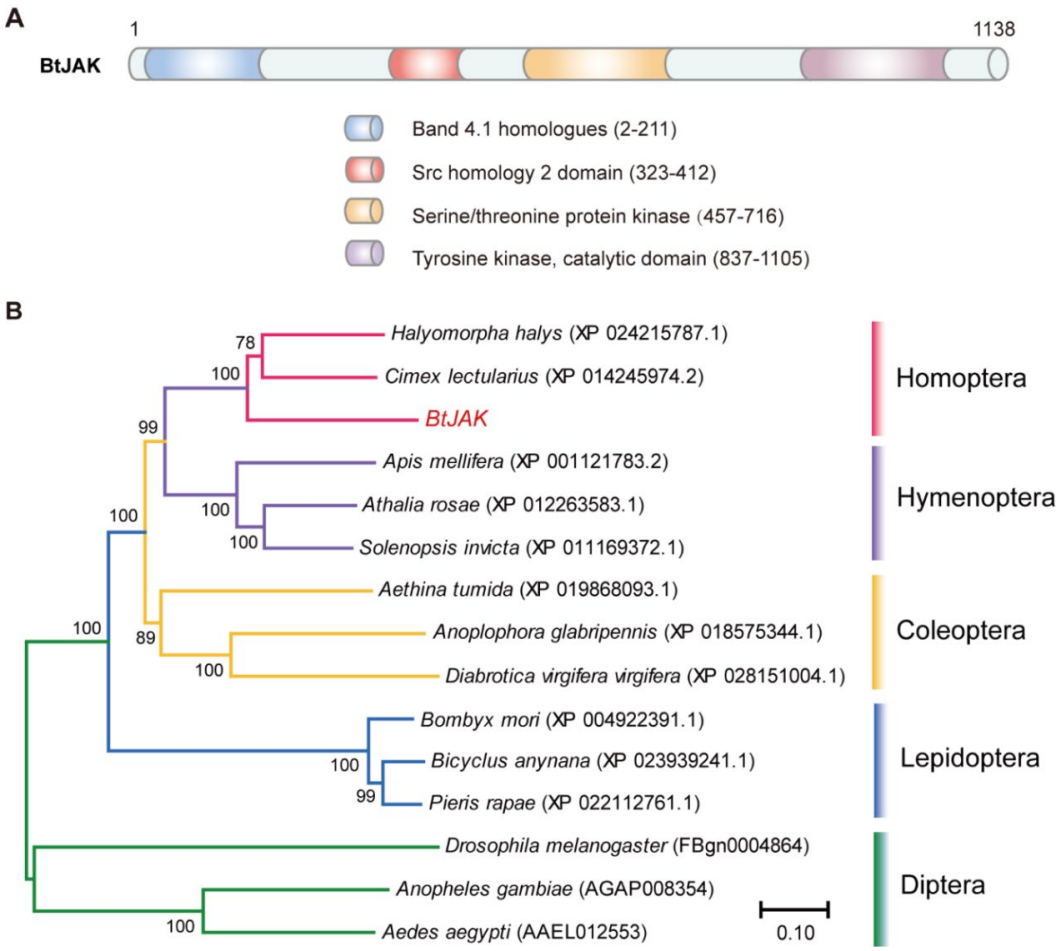

Fig. S8. Structural and phylogenetic analysis of BtJAK. (A) Schematic diagram showing the domain composition of BtJAK (Bta12850). The conserved domains were predicted using the SMART database. (B) Phylogenetic tree of JAKs from different insects. The phylogenetic tree was constructed using the neighbor-joining algorithm (MEGA7.0.14) from full sequence alignments computed in ClustalX. Bootstrap analysis (1000 replicates) was applied to evaluate the internal support for the tree topology.

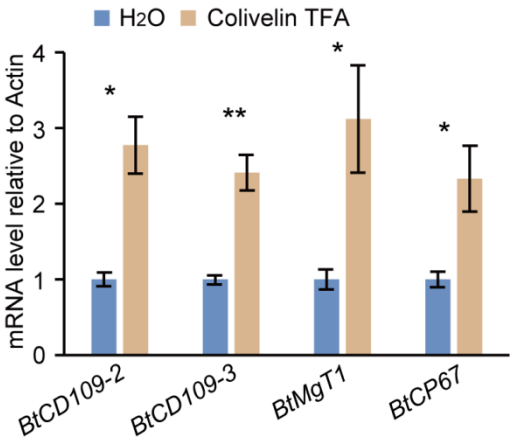

Fig. S9. Relative mRNA levels of BtSTAT-activated genes in non-viruliferous whiteflies after STAT activator (colivelin TFA) treatment. Mean ± SEM from three independent experiments with 40 whiteflies in each replicate. *$p < 0.05$, **$p < 0.01$ (independent-samples *t* test).

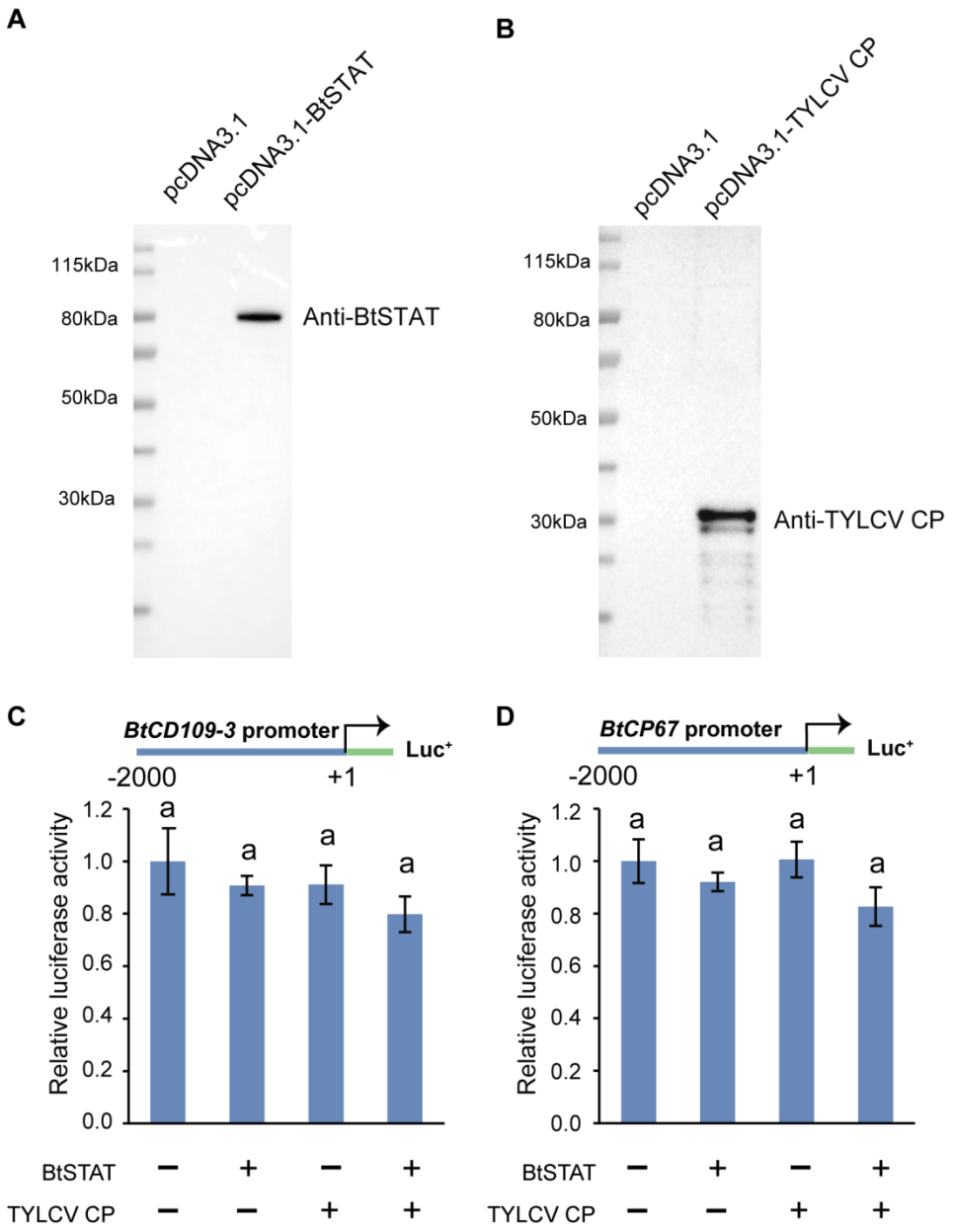

Fig. S10. Effects of BtSTAT and TYLCV CP overexpression on reporter activities in HEK293 cells. (A and B) Immunoblot analysis of the expression of BtSTAT (A) and TYLCV CP (B) in HEK293 cells. (C and D) Luciferase assays in HEK293 cells transfected with the expression vectors for BtSTAT and/or TYLCV CP, together with the reporter construct BtCD109-3_{2kb}-Luc (C) or BtCP67_{2kb}-Luc (D). Treatments with empty expression vector served as controls. A *Renilla* luciferase reporter construct was co-transfected in each well as a reference. Data represent normalized luciferase activity (firefly/*Renilla*) and are shown as mean ± SEM from three independent experiments. $p < 0.05$ (one-way ANOVA, LSD test).

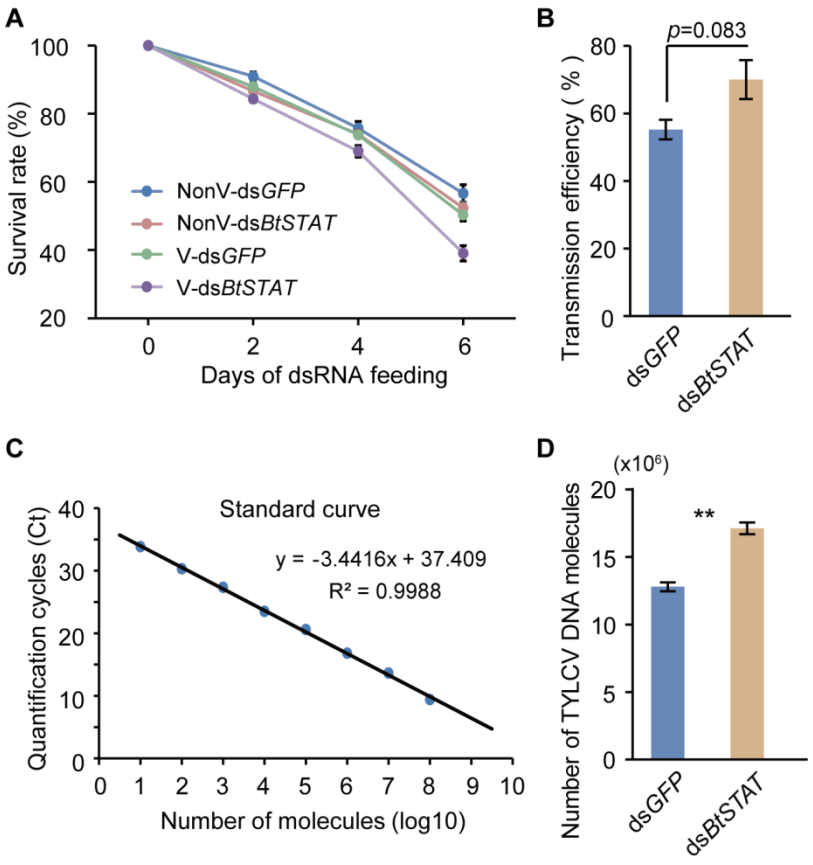

Fig. S11. Effect of silencing *BtSTAT* on whitefly fitness and virus transmission. (A) Survival rate of viruliferous (V) and non-viruliferous (NonV) whiteflies feeding on artificial diet containing ds*GFP* or ds*BtSTAT*. Data represent four biological replicates with 100 adults in each replication. (B-D) The percentage of test plants with virus genomic DNA (B) and absolute quantification of TYLCV DNA molecules in plants (C and D) at 30 days after inoculation by ds*GFP*- or ds*BtSTAT*-treated whiteflies. (C) Standard curve for absolute quantification of TYLCV DNA. Dilution series containing 10 and 10^8 copies of circular dsDNA plasmids carrying a full-length copy of the viral *CP* gene were used as quantification standards. Equation used for regression plot calculation is indicated. 9 to 10 plants per replicate and three replicates were used to calculate the disease incidence rate and viral DNA copies. *$p < 0.05$, **$p < 0.01$, (independent-samples *t* test).

Table S1. *Bemisia tabaci* orthologs of STAT downstream genes involved in insect response to immune challenge.

Species	Downstream genes	*Bemisia tabaci* orthologs			Identity	Presence of conserved functional domains*	Predicted STAT5B-binding site†
		Whitefly Genome ID	Genbank Accession	Description			
Drosophila melanogaster	*TotA* (AY035990.1)	-	-	-	-	-	-
	TotC (NM_080518.3)	-	-	-	-	-	-
	TotM (AY035992.1)	-	-	-	-	-	-
	Vir-1 (DQ143902.1)	-	-	-	-	-	-
	Tep1 (AJ269538.1)	Bta08339	XP_018897644.1	CD109 antigen-like (CD109-1)	33%	Yes	3
		Bta03341	XP_018913243.1	CD109 antigen (CD109-2)	19%	Yes	5
		Bta09750	XP_018898894.1	CD109 antigen-like (CD109-3)	17%	Yes	2
Aedes aegypti	*DVRF1* (AAEL008492)	Bta12654	XP_018901731.1	Membrane magnesium transporter 1 (MgT1)	56%	Yes	3
	DVRF2 (AAEL000896)	Bta12955	XP_018901879.1	Cuticle protein 67-like (CP67)	37%	Yes	3
		Bta13231	XP_018902407.1	Cuticle protein LPCP-23-like (LPCP23)	22%	Yes	4

*The conserved domains of proteins were predicted using the SMART database (http://smart.embl-heidelberg.de/)

†2 kb upstream DNA sequences were analyzed using the JASPAR database (http://jaspar.genereg.net/)

Table S2. Primers used in this study.

Primer		Sequences(5'-3')	Length	Purpose
pGBKT7-TYLCV CP	F	GGGAATTCCATATGATGTCGAAGC	797bp	Expression of TYLCV CP in Y2H Gold (EcoRI sites are underlined)
	R	CCGGAATTCTTAATTTGATAT		
pGEX-6p-1-TYLCV CP	F	CGGGATCCATGTCGAAGCGACCAGGCGA	793bp	Expression of TYLCV CP in *E. coli* (BamH I and EcoR I sites are underlined)
	R	CGGAATTCTTAATTTGATATTGAATCAT		
pAc5.1/V5-BtSTAT	F	CGGAATTCTATGGCCTTGTGGATGAAAGC	2291bp	Expression of BtSTAT in S2 cells (EcoRI and XbaI sites are underlined)
	R	GCTCTAGACTCAATGTTACTAACCTGGCAA		
pET28a-BtSTAT	F	CGGAATTCATGGCCTTGTGGATGAAAGC	615bp	Expression of BtSTAT in *E. coli* (EcoRI and SacI sites are underlined)
	R	CGAGCTCTTAGTTTTCAGATGATGATTGAAA TTCC		
qTYLCV	F	GAAGCGACCAGGCGATATAA	189 bp	qPCR for TYLCV total DNA
	R	GGAACATCAGGGCTTCGATA		
TYLCV	F	ATACCTGGACACCTAATGGC	413 bp	TYLCV DNA detection
	R	AGTCACGGGCCCTTACA		
q-β-actin	F	TCTTCCAGCCATCCTTCTTG	173bp	q(RT)-PCR for *β-actin*
	R	CGGTGATTTCCTTCTGCATT		
qBtDOME	F	CAGTGCGAGGGAATTTCTACA	136bp	qRT-PCR for *BtDOME*
	R	ACACCATACCACTGCTTCCA		
qBtJAK	F	TTGATGAGCTTGCACCAAAT	138bp	qRT-PCR for *BtJAK*
	R	TTCCTTCAAAGCACATCCTG		
qBtSTAT	F	CCATTTCACTGTTGGTGGAG	150bp	qRT-PCR for *BtSTAT*
	R	AACGGTATACGCCCAAGTTC		
qCD109-1	F	TCCCAATGGTAGCACATGGT	123bp	qRT-PCR for *CD109-1*
	R	GCTTGGTTGTTTGAGAGCCA		
qCD109-2	F	TCATTTGGCGTGAAGGCTTG	170bp	qRT-PCR for *CD109-2*
	R	TCGTTGAGAAGCGTCCATTT		
qCD109-3	F	ACCTGGCAACCCAATCAAAC	125bp	qRT-PCR for *CD109-3*
	R	CATCTCGCAGCAGAAACACA		
qMgT1	F	AGCCACTGTGGATCTGGAAA	112bp	qRT-PCR for *MgT1*
	R	TGACGCAGGATCAAATTCCG		
qCP67	F	CCCGCAGCTCTACTACTCG	57bp	qRT-PCR for *CP67*
	R	CGGAGGATGTTGGAGGACTG		
qLPCP23	F	GATACGGAGCTGGTTACGGA	68bp	qRT-PCR for *LPCP23*
	R	AGCGTATGAGGAGACGTAGC		
pcDNA3.1-BtSTAT	F	GGGGTACCTATGGCCTTGTGGATGAAAGC	2291bp	Expression of BtSTAT in 293T cells (KpnI and EcoRI sites are underlined)
	R	GGAATTCTTACAATGTTACTAACCTGGCAA		
pcDNA3.1-TYLCV CP	F	GGGGTACCTATGTCGAAGCGACCAGGCGA	792bp	Expression of TYLCV CP in 293T cells (KpnI and EcoRI sites are underlined)
	R	GGAATTCTTAATTTGATATTGAATCATAGAAA TAGATG		
pGL3-CD109-2	F	CTAGCTAGCGACCTGAAAAACACAAAATAAT GCT	2000bp	Construction of pGL3-basic reporter vector (NheI and SmaI sites are underlined)

	R	TCCCCCGGGTACACGAAGGACGAAGGAGC		
pGL3-CD109-3	F	CTAGCTAGCCGGACATGCAATTTTTGACT	2000bp	Construction of pGL3-basic reporter vector (NheI and SmaI sites are underlined)
	R	TCCCCCGGGCGGCCTGACAGAAGCGACTG		
pGL3-MgT1	F	CTAGCTAGCTAAATTTGTGGTTTTTCACCCCC	2000bp	Construction of pGL3-basic reporter vector (NheI and SmaI sites are underlined)
	R	TCCCCCGGGGGTTATGTTATGATTGTTGTTGTTGTC		
pGL3-CP67	F	CTAGCTAGCAAACACCCATGGGATTACCT	2000bp	Construction of pGL3-basic reporter vector (NheI and SmaI sites are underlined)
	R	TCCCCCGGGCGTTCCACGGCCAGAGAAGC		
dsRNA-GFP	F	T7-CTCGTGACCACCCTGACCTAC	247 bp	*GFP* dsRNA synthesis
	R	T7-GTTCACCTTGATGCCGTTCTT		
dsRNA-BtDOME	F	T7-GTCCCATCATCAACTTGCAG	226bp	*BtDOME* dsRNA synthesis
	R	T7-CTGCTTCCAGAGTGGTTTCA		
dsRNA-BtJAK	F	T7-GAAACTCTGAGCAGCCATGA	255bp	*BtJAK* dsRNA synthesis
	R	T7-ACTGCTACTCCGCTCCAAAT		
dsRNA-BtSTAT	F	T7-CCTCATTGCAAAGCCGCATA	216bp	*BtSTAT* dsRNA synthesis
	R	T7-TAGTCGTTCCGCCTCTTTGA		
dsRNA-CD109-2	F	T7-CAGCAGCAGAAGTTGGACTC	220bp	*CD109-2* dsRNA synthesis
	R	T7-AATTGGCAGGTATCGGGACA		
dsRNA-CD109-2(2)	F	T7-AGTTCCTGTTCGTCTTGGAGA	285bp	*CD109-2* dsRNA synthesis
	R	T7-GGAAAGATTGGGCCGACAAC		
dsRNA-CD109-3	F	T7-AAACACCGCTTTCACTTGGG	310bp	*CD109-3* dsRNA synthesis
	R	T7-TGGGAAATCTCTGGTGTACCT		
dsRNA-CD109-3(2)	F	T7-CAGAGCTGCTGAAGCTGAAA	263bp	*CD109-3* dsRNA synthesis
	R	T7-GTCAAATGAATCCGAACCCGG		
dsRNA-MgT1	F	T7-GTTAATCACCGTGGCAGAGC	306bp	*MgT1* dsRNA synthesis
	R	T7-GTTCCCAGTGAATGTGAGGC		
dsRNA-CP67	F	T7-TAGCCACCTACCACGCCCCG	172bp	*CP67* dsRNA synthesis
	R	T7-GTACGTAATGGGCTCCGAA		

*T7, 5´-TAATACGACTCACTATAGG- 3´

Table S3. The amplification efficiency of primers used in quantitative PCR analysis.

Primer		Sequences(5'-3')	Amplification efficiency（%）	R^2
qTYLCV	F	GAAGCGACCAGGCGATATAA	95.24	0.9988
	R	GGAACATCAGGGCTTCGATA		
q-β-actin	F	TCTTCCAGCCATCCTTCTTG	96.41	0.9913
	R	CGGTGATTTCCTTCTGCATT		
qBtDOME	F	CAGTGCGAGGGAATTTCTACA	97.40	0.992
	R	ACACCATACCACTGCTTCCA		
qBtJAK	F	TTGATGAGCTTGCACCAAAT	96.95	0.9924
	R	TTCCTTCAAAGCACATCCTG		
qBtSTAT	F	CCATTTCACTGTTGGTGGAG	98.09	0.9985
	R	AACGGTATACGCCCAAGTTC		
qCD109-1	F	TCCCAATGGTAGCACATGGT	93.23	0.9991
	R	GCTTGGTTGTTTGAGAGCCA		
qCD109-2	F	TCATTTGGCGTGAAGGCTTG	96.55	0.9968
	R	TCGTTGAGAAGCGTCCATTT		
qCD109-3	F	ACCTGGCAACCCAATCAAAC	97.07	0.9911
	R	CATCTCGCAGCAGAAACACA		
qMgT1	F	AGCCACTGTGGATCTGGAAA	97.35	0.9897
	R	TGACGCAGGATCAAATTCCG		
qCP67	F	CCCGCAGCTCTACTACTCG	95.50	0.989
	R	CGGAGGATGTTGGAGGACTG		
qLPCP23	F	GATACGGAGCTGGTTACGGA	97.77	0.9888
	R	AGCGTATGAGGAGACGTAGC		

Table S4. The amino acid sequence similarities between *Drosophila melanogaster* Teps and *Bemisia tabaci* CD109s

	DmTep1	DmTep2	DmTep3	DmTep4	DmTep5*	DmTep6
BtCD109-1	32.83%	**37.43%**	37.03%	30.4%	-	21.54%
BtCD109-2	18.36%	20.71%	20.25%	18.84%	-	**56.84%**
BtCD109-3	16.82%	18.47%	17.61%	17.33%	-	**27.25%**

* DmTep5 is a pseudogene.

Table S5. A summary of the online prediction programs and results of BtCD109-2 and BtCD109-3.

Protein name	Signal peptide*	GPI anchor site†	
	SignalP 6.0 (likelihood)	PredGP	GPI-SOM
BtCD109-2	Yes(0.9997)	Probable	Yes
BtCD109-3	Yes(0.9355)	Not GPI-anchored	Yes
CD109 (*Homo sapiens*)	Yes(0.9997)	Highly probable	Yes

*The SignalP 6.0 online program (https://services.healthtech.dtu.dk/service.php?SignalP) was used for the prediction of the presence of a signal peptide

†Two online programs, PredGP (http://gpcr2.biocomp.unibo.it/gpipe/index.htm) and GPI-SOM (http://gpi.unibe.ch/), were used for the prediction of GPI-anchored proteins